applied sciences

MDPI

Article

Mechanical Properties and Corrosion Resistance of TiAl6V4 Alloy Produced with SLM Technique and Used for Customized Mesh in Bone Augmentations

Nicola De Angelis [1,2,3,*], Luca Solimei [1,2], Claudio Pasquale [1,2], Lorenzo Alvito [4], Alberto Lagazzo [4] and Fabrizio Barberis [4]

[1] Department of Surgical Sciences and Integrated Diagnostics, University of Genova, 16126 Genova, Italy; lucasolimei@hotmail.it (L.S.); clodent@gmail.com (C.P.)
[2] Department of Mechanical and Energetics Engineering, University of Genova, 16126 Genova, Italy
[3] Department of Dentistry, University of Technology MARA Sungai Buloh Malaysia, Shah Alam 40450, Malaysia
[4] Department of Civil, Chemical and Environmental Engineering, University of Genova, 16126 Genova, Italy; l.alvito96@gmail.com (L.A.); alberto.lagazzo@unige.it (A.L.); fabrizio.barberis@unige.it (F.B.)
* Correspondence: nicolaantonio.deangelis@edu.unige.it; Tel.: +39-347-4188-180

Abstract: Bone augmentation procedures represent a real clinical challenge. One option is the use of titanium meshes. Additive manufacturing techniques can provide custom-made devices in titanium alloy. The purpose of this study was to investigate the material used, which can influence the outcomes of the bone augmentation procedure. Specific test samples were obtained from two different manufacturers with two different shapes: surfaces without perforations and with calibrated perforations. Three-point bending tests were run as well as internal friction tests to verify the Young's modulus. Test samples were placed in two different buffered solutions and analyzed with optical microscopy. A further SEM analysis was done to observe any microstructural modification. Three-point flexural tests were conducted on 12 specimens. Initial bending was observed at lower applied stresses for the perforated samples (503 MPa) compared to non-perforated ones (900 MPa); the ultimate flexural strength was registered at 513 MPa and 1145 MPa for perforated and non-perforated samples, respectively. Both microscopic analyses (optical and SEM) showed no significant alterations. Conclusions: A normal masticatory load cannot modify the device. Chemical action in the case of exposure does not create macroscopic and microscopic alterations of the surface.

Keywords: alveolar bone defects; guided bone regeneration; titanium meshes; customized titanium meshes; laser melting process; electron beam melting

Citation: De Angelis, N.; Solimei, L.; Pasquale, C.; Alvito, L.; Lagazzo, A.; Barberis, F. Mechanical Properties and Corrosion Resistance of TiAl6V4 Alloy Produced with SLM Technique and Used for Customized Mesh in Bone Augmentations. *Appl. Sci.* **2021**, *11*, 5622. https://doi.org/10.3390/app11125622

Academic Editor: Vittorio Checchi

Received: 11 May 2021
Accepted: 15 June 2021
Published: 18 June 2021

1. Introduction

The use of dental implants is a very common procedure [1]. For ideal prosthetic design, implants must be inserted in a correct 3D plan [2]. Patients may present alveolar ridge defects as a consequence of periodontal disease, dental trauma, traumatic extraction, or genetic anomalies, which do not allow the correct implant position [3,4].

Different treatment options have been described to reconstruct these defects, which may include inlay and onlay block bone grafts, crestal splitting, osteogenetic distraction, and guided bone regeneration (GBR) using resorbable and non-resorbable barrier membranes [5]. Of these, GBR seems to be the most reliable and predictable, providing excellent long-term stability [6,7].

The basic principle of GBR involves placing a mechanical barrier to protect the blood clot and to isolate the bony defect from the surrounding connective and epithelial tissue invasion. This space is needed to allow the osteoblasts to access the space intended for bone regeneration. The use of a barrier membrane, especially a resorbable one, has the

advantage of facilitating the procedure, but often the shape of the defect itself may create a collapse of the barrier and the loss of the "space maintaining" effect [8].

Titanium meshes, as an alternative to membranes, have been used for a long time as a predictable technique for bone regeneration and, owing to their rigidity, the adaptation onto the defect and maintenance of their shape can be more stable [9]. To overcome the main drawbacks, which are the remaining sharp margins after cutting and the increased surgical time required for their shaping and fitting, pre-shaping of the mesh on a stereolithographic model (STL) of the patient's jaw can be an alternative to significantly shorten the intraoperative time, but with a significant cost increase [10]. More recently, 3D-printed, custom-made titanium devices have been introduced as a modern alternative [11].

Regardless of the production technique for any implantable devices, it is mandatory to control the characteristics to optimize their biological performance [12]. The stiffness of titanium meshes can damage the soft tissue, and the mechanical strength is related to the thickness of the material and pore dimensions. More specifically, the surface properties direct the cellular interactions [13]. These properties, including surface topography and chemical composition, are usually derived by the surface treatments applied [14].

Surface topography and roughness are aspects that can be easily manipulated by post-production surface treatments and that play a strategic role in the determination of cellular interactions, influencing adhesion and differentiation [15,16]. High degrees of roughness represent a major risk for ionic leakage from the material [17] and the bacterial adhesion can be increased, with the consequence of implant failures [18].

Smooth surfaces are able to reduce the biological processes at the interface, keeping the titanium oxidized layer properties unaffected for periods [16]. Thus, the correct micro- and nano-roughness levels can stimulate osteoblast differentiation and maturation, proliferation, and production of both matrices [19]. Although the mesh characteristics should be highly controlled, it is important to note that the biological response depends also on the correct diagnosis and clinical indication. Moreover, if an exposure during the healing phase occurs, it is relevant to demonstrate if, beside the unfavorable outcome, chemical modifications of the exposed surface may affect the bone growth.

The present study investigated two different commercial customized devices, comparing their mechanical properties (flexion test and internal friction) and their macro- and microstructural changes after exposure to different degrees of pH to observe if the modifications of the material were coherent with the clinical findings. Further evaluations were made using SEM with profiles analysis and chemical composition.

2. Materials and Methods

2.1. Samples' Preparation

Specific test samples produced with the laser sintering technique used for customized implantable titanium meshes were obtained from two different manufacturers, BoneEasy (Arada, Ovar, Portugal) and BTK (Vicenza, Italy), and came with two different shapes: surfaces without perforations and with calibrated perforations 1.2 mm in diameter.

The samples were characterized by the following dimensions: 40 mm length, 10 mm width, and 0.5 mm thickness, to conduct the test according to the protocols of ISO5832-3:2014, ASTM F136:2013, ASTM F2934:2014, ASTM F3001:2014, and ASTM B348:2013.

The chemical composition declared by the manufacturer was TiAl6V4 with the following percentages of the different elements: Al 5.5–6.5% and V 3.5–4.5%.

All the tests were conducted on:

- Three BoneEasy specimens (BE) without perforations,
- Three Biotek specimens (BTK) without perforations,
- Three BoneEasy specimens (BE) with perforations, and
- Three Biotek specimens (BTK) with perforations.

2.2. Experiments

In order to simulate the mechanical stress due to the masticatory function over the implanted device, three-point bending tests were run as well as internal friction tests to verify the Young's modulus.

The bending tests were performed using a Zwick/Roell Z0.5 electromechanical testing machine (Standards EN 2562–EN 2746) equipped with a three-point bending device with a span of 40 mm. All the tests were run on rectangular samples 0.5 mm in thickness, 10 mm in width, and 40 mm in length, at a rate of 5 mm/min for the determination of the flexural elastic modulus and a rate of 30 mm/min until break.

The tests for the determination of the internal friction were performed using an experimental setup consisting of a laser vibrometer to measure the displacement of a sample placed on two supporting pins and impulsively hit by a ball and on an oscilloscope to evaluate the resonance frequency. The physics equation that links the geometric parameters of the specimen and its Young's Modulus E' to the material frequency is:

$$f = \frac{\lambda^2 \cdot 10^6}{2\pi L^2}\left(\frac{Eh^2}{12\rho}\right)^{1/2}$$

where E is the Young's Modulus [Gpa], the density is [g/cm^3], h is the specimen thickness [mm], L is the span between the two supports [mm], and λ is the modal coefficient equal to 4.73.

The speed c_o of the elastic longitudinal waves along the bar, expressed in m/s, can be derived as:

$$c_o = \frac{2\pi f L^2}{\lambda^2 r \cdot 10^3}$$

where = $h/(12)^{0.5}$ is the radius of inertia of the sample section [mm]. The Young's Modulus can be calculated through the equation:

$$E = {c_o}^2\, 10^{-6}$$

$$Q^{-1} = \frac{1}{\pi f \Delta t}\ln\left(\frac{A_1}{A_2}\right)$$

To reproduce the chemical oral environment with consistent pH variations (food, beverages, and existing pathologies), the test samples were placed into two different buffered solutions at pH 7 and pH 4 and analyzed with optical microscopy (50, 100×) at 7, 14, and 21 days.

2.3. Analysis

A further SEM analysis was done to assess whether different chemical baths could produce external and internal modifications of the alloy structures and also to analyze the composition of the specimens, comparing these with the manufacturer's declarations by means of Specific Energy-dispersive X-ray spectroscopy.

Samples without perforations produced by both companies were cut and incorporated into epoxy resin for inspection of their profiles using SEM and mathematical calculation (Image J and MATLAB software) of the roughness parameters.

3. Results

Three-point flexural tests were conducted on 12 specimens (Figure 1).

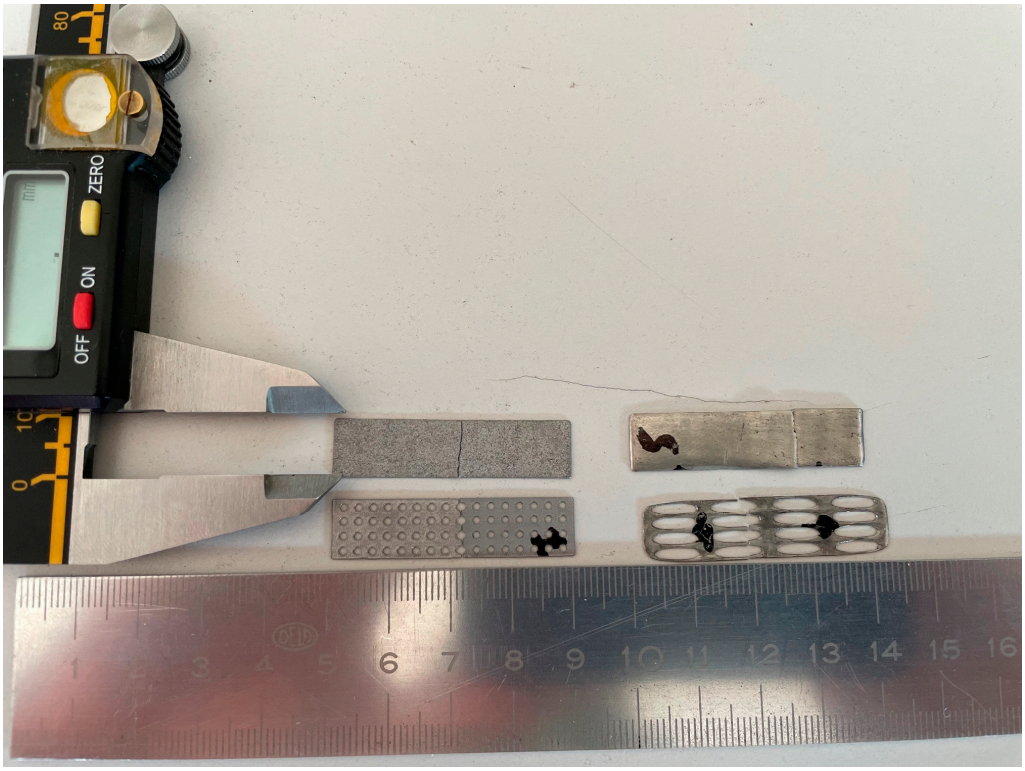

Figure 1. Four of the specimens used for the investigation. Perforated and non-perforated BTK and BoneEasy. The picture was taken after the three-point flexural tests, and it is evident of the fracture of the specimen.

Initial bending was observed at lower applied stresses for perforated samples (503 MPa) compared to non-perforated ones (900 MPa). The ultimate flexural strength was registered at 513 MPa and 1145 MPa for the perforated and non-perforated samples, respectively (Figure 2).

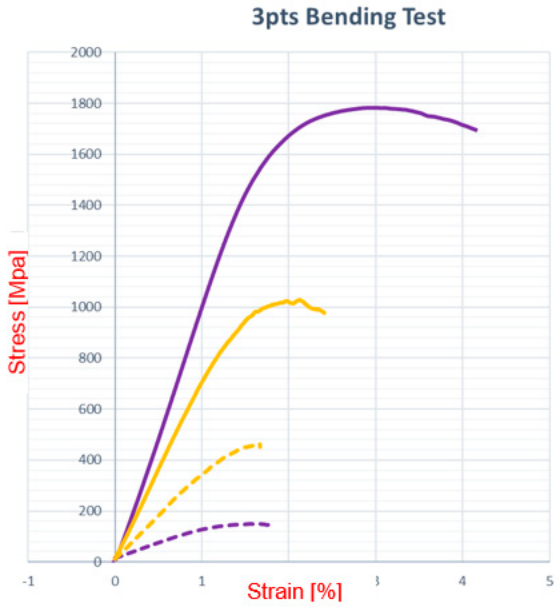

Figure 2. Diagram of three-point flexural strength on four different types of specimens.

Internal friction tests were conducted to determine the Young's modulus, which was reported from 101 to 107 MPa (Figure 3).

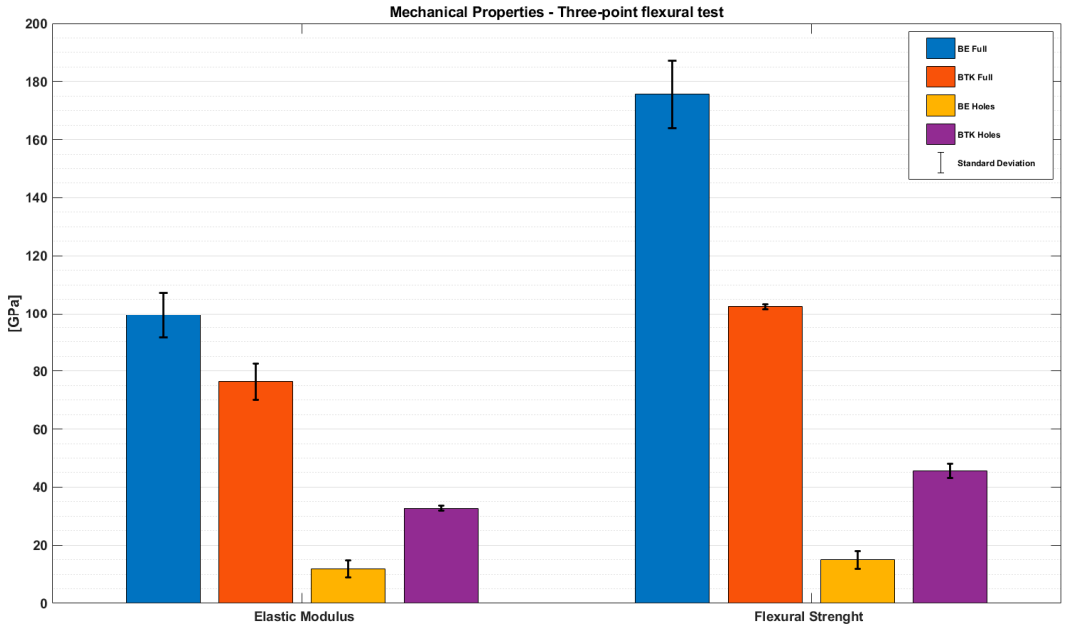

Figure 3. Graphical representation of elastic modulus and flexural strength values on the four types of specimens.

The analysis with an optical microscope at different pH at 7, 14, and 21 days, respectively, did not reveal any macroscopic alteration of the surface (Figure 4).

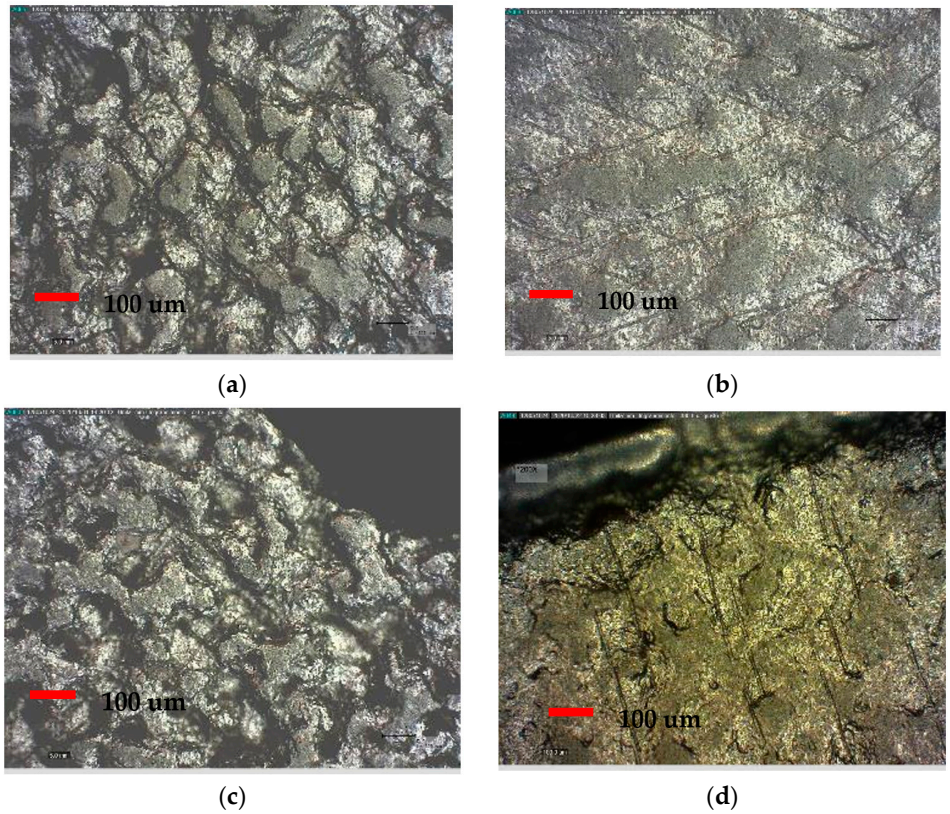

(**a**) (**b**)

(**c**) (**d**)

Figure 4. A 200× optical microscopy analysis: (**a**,**b**) on specimens exposed at pH 7 for 21 days, (**c**,**d**) on specimens exposed at pH 4 for 21 days. No macroscopic differences can be seen.

The further SEM analysis done on all the samples showed several microscopic defects of the surface on all the samples exposed at pH 4. Thus, it can be concluded that those imperfections are attributed to a corrosion effect (Figure 5).

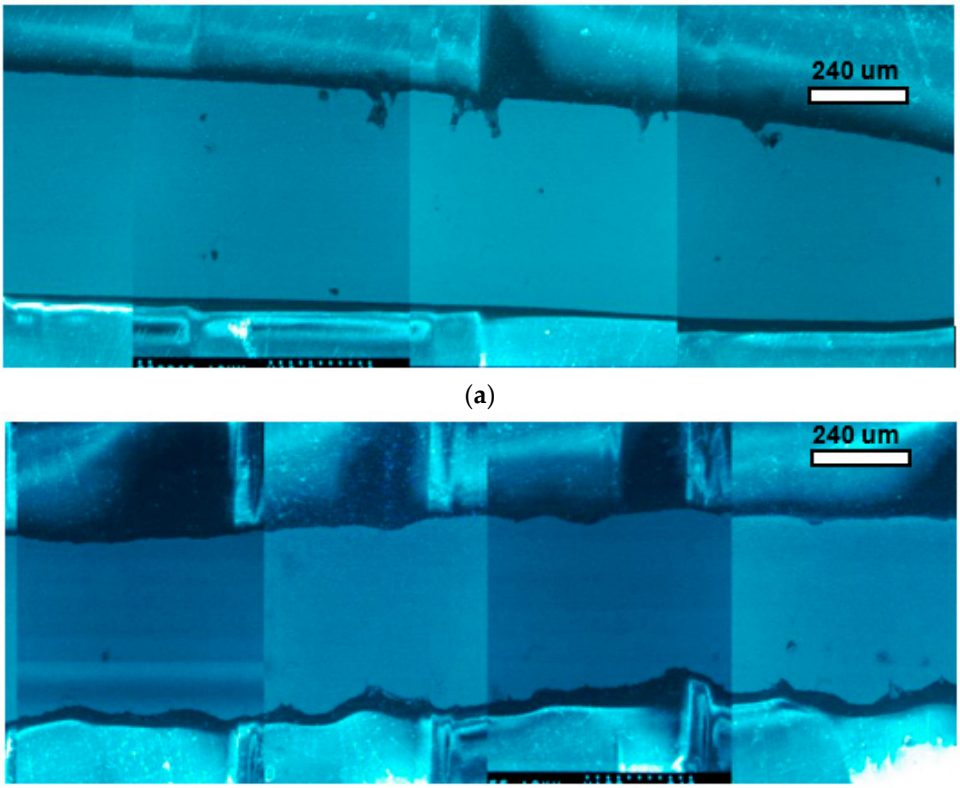

(**a**)

(**b**)

Figure 5. SEM analysis revealed profile and internal defects on both BoneEasy (**a**) and BTK (**b**) samples, probably attributed to the long exposure to a pH 4 buffered solution.

The roughness parameters Ra, Rq, and Sigma of the samples are reported in Tables 1 and 2, where Ra is the roughness average, Rq the root mean square, and Sigma is the standard deviation.

The profile analysis of the lower faces of the BE and BTK specimens at pH 7 showed Sigma values (σ) of 1.165 µm and 21.555 µm, respectively. On the upper face, the same samples showed Sigma values (σ) of 1.697 µm for BE and 13.756 µm for BTK.

After pH 4 immersion, the lower faces of the BE and BTK specimens showed Sigma values (σ) of 0.883 µm and 19.685 µm, respectively. The upper faces of the same samples had Sigma values (σ) of 1.583 µm for BE and 9.073 µm for BTK.

The Sigma values confirmed that the BTK samples were rougher than the BE ones and also that the BTK ones had two different surfaces with different degrees of roughness (Tables 1 and 2, Figure 6).

Table 1. Roughness parameters on lower faces of both samples. The numbers of samples used for the analysis are identified in each column.

Lower Face	BTK 7	BTK 4	BE 7	BE 4
Ra	17.673 µm	15.636 µm	1.466 µm	1.126 µm
Rq	21.553 µm	19.683 µm	1.945 µm	1.474 µm
Sigma	21.555 µm	19.685 µm	1.165 µm	0.883 µm

Table 2. Roughness parameters on upper faces of both samples.

Upper Face	BTK 7	BTK 4	BE 7	BE 4
Ra	12.125 µm	7.601 µm	2.387 µm	2.103 µm
Rq	13.754 µm	9.072 µm	2.833 µm	2.644 µm
Sigma	13.756 µm	9.073 µm	1.697 µm	1.583 µm

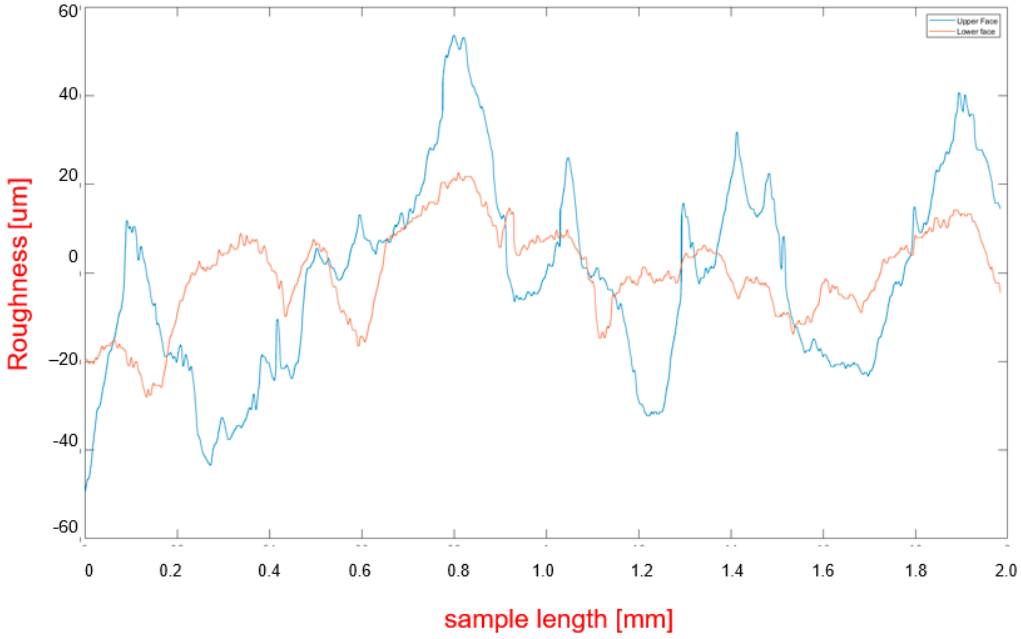

Figure 6. Profile analysis of upper and lower faces.

The profile analysis revealed, also, some internal defects, and the further Energy-dispersive X-ray spectroscopy evidenced the chemical composition of both samples, in which high percentages of carbon were detected (1.25% for BE and 3.65% for BTK) (Figures 7 and 8).

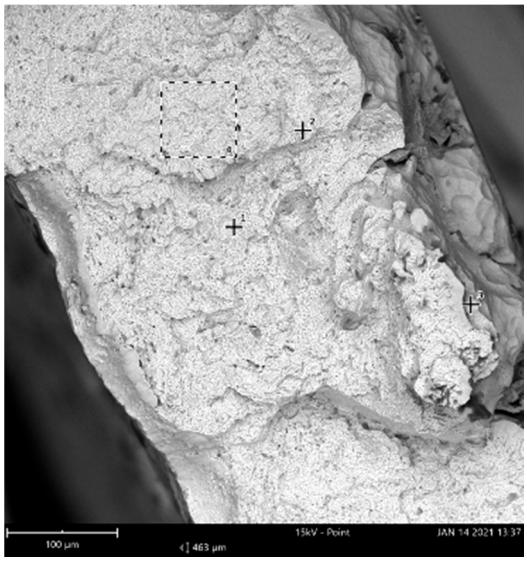

(**a**)

Figure 7. *Cont.*

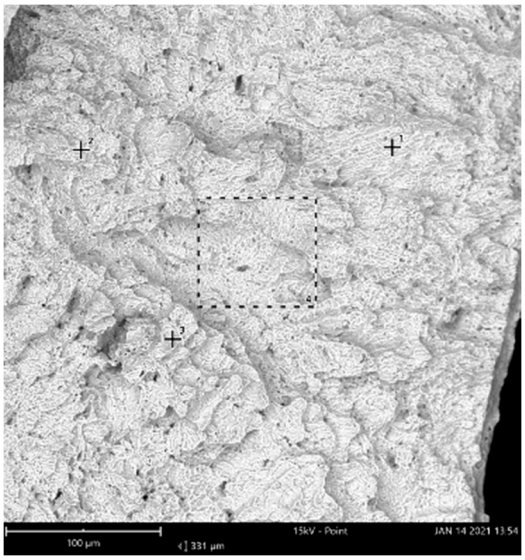

(**b**)

Figure 7. SEM internal defects on BTK (**a**) and BE (**b**) samples.

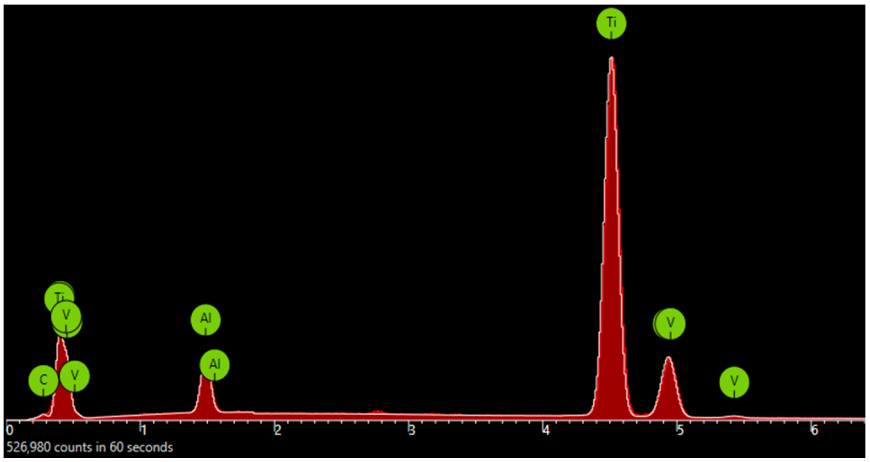

(**a**)

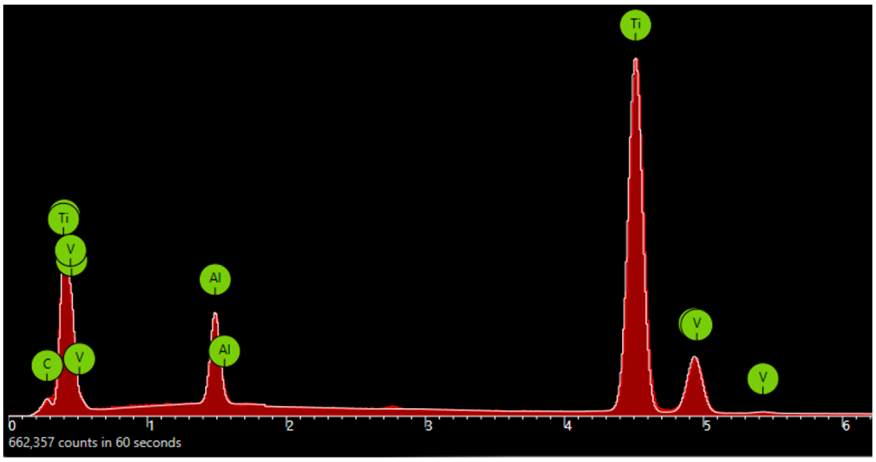

(**b**)

Figure 8. Energy-dispersive X-ray spectroscopy on BE samples (**a**) and BTK samples (**b**). *X*-axis represents the energy (KeV) and *Y*-axis represents the number of counts. The highest peak is titanium but an average of 1.25% and 3.65% of carbon can be detected in the BE and BTK samples, respectively.

4. Discussion

Additive manufacturing (AM) is widely applied in the medical field and it is becoming popular in oral surgery. However, only a few studies have analyzed the effect of the laser melting and sintering process (defined as additive manufacturing techniques) on the metal alloys in terms of mechanical and chemical properties [20,21].

Considering that the implant has to be placed in the oral cavity, a variety of factors can influence the final outcome: masticatory function and applied stress on the device, chemical action of the saliva, and, in the case of partial exposure, of foods and beverages, including also any endogenous pathologies, like gastro-esophageal acid reflux.

AM technology offers some advantages compared to conventional techniques [22], such as digital planning and design of the customized mesh, shorter surgical times, and easy adaptation of the device to the bone defect [23–26].

Otawa et al. [27] evaluated the dimensional accuracy of customized AM Ti mesh. The thickness of the polished device was 0.3 mm with perforations of 1.0 mm. The results obtained demonstrated that the *x*- and *y*-axes representation showed higher accuracy compared to the *z*-axis. The mean accuracy error value reported was 139 µm.

Sumida et al. [28] compared the clinical performance of customized AM with conventional Ti meshes for bone augmentation procedures in 26 patients. The customized AM meshes were manufactured with a thickness of 0.5 mm and with 1.0-mm diameter pores. The screw perforations for positioning the AM mesh had a 1.5-mm diameter, and the mesh was manually polished until 0.3-mm thickness was achieved. During implant placement, the Ti meshes were positioned with autogenous bone. The authors reported a higher surgical time for conventional Ti mesh compared to customized AM mesh. Furthermore, conventional meshes were associated with 15.4% of mucosal dehiscence with infection compared to AM procedures.

Inoue et al. [29] evaluated the feasibility of the customized Ti mesh sheets for alveolar bone reconstruction in two patients. A customized SLM Ti mesh sheet was positioned at the same time as placing a commercial implant.

None of the abovementioned studies investigated whether the additive manufacturing process may influence the mechanical properties. From the results of this study, there is a clear difference between perforated and non-perforated samples, with an obvious higher resistance, calculated as ultimate flexural strength, for the samples without any kind of perforation.

An adult human male can produce an occlusal force that averages from 45–68 kg (441.3–666.8 MPa) on molar sites. The values of the ultimate flexural strength for non-perforated samples are much higher, but perforated samples break at 503 MPa and start bending with alteration of the initial shape at 300 MPa. The samples, both perforated and not, from BoneEasy (BE) seem to have a higher resistance than the BTK ones. The elastic modulus of perforated samples is lower than the full samples and more similar to the bone's Young's modulus (10–20 GPa). Although the shape of the customized mesh was different from the samples, with a noticeable difference also of the mechanical properties, this aspect should be considered after the implantation in order to avoid potentially dangerous stresses on the device.

Partial exposure of the mesh is one of the most common complications and it has been demonstrated by several studies that it may average from 0 to 66% [28], regardless of the site and the extension of the bone augmentation.

The existing evidence does not report whether the part exposed to the oral cavity and, thus, to contaminants such as food and beverages but also to sudden and extremely variable chemical conditions, may influence or not the surface of the device, affecting the bone response.

In this study, several conditions were simulated, from the immersion of the sample in saline solution (pH 7) up to the extreme acid buffering with pH 4 for a maximum time of 21 days. The microscopic analysis revealed different Sigma values (standard deviation) for the two examined samples, which was most evident after the immersion in the acid

solution. Moreover, the samples from BoneEasy were apparently smoother than the BTK ones and this aspect could imply a lower bacterial adhesion in the case of complications.

The effect of the acid solution, although not reproducible in humans, revealed that both samples were extremely resistant, but the surface showed a moderate corrosion, which was analyzed with SEM and with energy-dispersive X-ray spectroscopy. The presence of high percentages of carbon represents an important and negative aspect, which was found in all samples, with slight differences between the two manufacturers.

Several reasons could be addressed to explain these values, and during the investigations none of the examined bars was touched without gloves, in order to eliminate the superficial contamination of the human epithelial cells. Furthermore, the same values of carbon were detected also from the analysis of the internal margin immediately after the fracture of the sample.

In a recent article, Cruz et al. [29] compared three different types of meshes from BTK, BoneEasy, and Reoss. The result of their profile analysis was coherent with the data retrieved in this investigation. They also found several artifacts embedded into the meshes. Specifically, several deep cracks were found, and it can be assumed that these features existed already after the first production steps of the mesh. The EDS analysis revealed that the embedded residues were aluminum and oxygen. These alterations of the surface were probably induced by the post-production alumina (Al2O3) sandblasting process. Apparently, the presence of carbon in both the BTK and BoneEasy samples could not be explained and this undoubtedly represented a certain weakness in the production of these devices. It would be important to understand whether the same findings can be observed also in patients' dedicated meshes, in order to clarify the safety of their use.

5. Conclusions

Within the limitations of this study, it can be assessed that a normal masticatory load cannot modify the device. Mechanical tests revealed that the BE- and BTK-manufactured samples had different responses to the applied stress, and the elastic modulus was significantly lower for perforated samples, with differences between BE and BTK, which showed a value more similar to the Young's modulus of the bone. Chemical action in the case of exposure did not cause macroscopic and microscopic alteration of the surface. Thus, besides the unfavorable clinical outcome, it can be assumed that no structural modifications are expected. It can be concluded that TiAl6V4 is a stable and promising material for customized devices, but more clinical studies are needed to understand the long-term host responses.

Author Contributions: Conceptualization, N.D.A. and L.S.; methodology, N.D.A., F.B. and A.L.; software, L.A. and A.L.; validation, C.P., L.S. and N.D.A.; formal analysis, L.A.; investigation, L.A. and N.D.A.; resources, F.B.; data curation, L.A.; writing—original draft preparation, N.D.A.; writing—review and editing, N.D.A. and A.L.; visualization, L.A.; supervision, F.B.; project administration, F.B. All authors have read and agreed to the published version of the manuscript.

Funding: This research received no external funding.

Institutional Review Board Statement: Not applicable.

Informed Consent Statement: Not applicable.

Data Availability Statement: Not applicable.

Conflicts of Interest: The authors declare no conflict of interest.

References

1. Smeet, R.; Stadlinger, B.; Frank, S. Impact of dental implant surface modifications on osseointegration. *Biomed. Res. Int.* **2016**, *2*, 1–16. [CrossRef]
2. Buser, D.; Martin, W.; Belser, U.C. Optimizing esthetics for implant restorations in the anterior maxilla: Anatomic and surgical considerations. *Int. J. Oral Maxillofac. Implant.* **2004**, *19*, 43–61.

3. Jegham, H.; Masmoudi, R.; Ouertani, H.; Blouza, I.; Turki, S.; Khattech, M. Ridge augmentation with titanium mesh: A case report. *J. Stomatol. Oral Maxillofac. Surg.* **2017**, *118*, 181–186. [CrossRef] [PubMed]
4. Rocchietta, I.; Fontana, F.; Simion, M. Clinical outcomes of vertical bone augmentation to enable dental implant placement: A systematic review. *J. Clin. Periodontol.* **2008**, *35*, 203–215. [CrossRef] [PubMed]
5. Rakhmatia, Y.D.; Ayukawa, Y.; Furuhashi, A.; Koyano, K. Current barrier membranes: Titanium mesh and other membranes for guided bone regeneration in dental applications. *J. Prosthodont. Res.* **2013**, *57*, 3–14. [CrossRef] [PubMed]
6. Li, H.; Zheng, J.; Zhang, S.; Yang, C.; Kwon, Y.-D.; Kim, Y.-J. Experiment of GBR for repair of peri-implant alveolar defects in beagle dogs. *Sci. Rep.* **2018**, *8*, 16532. [CrossRef]
7. Donos, N.; Kostopoulos, L.; Tonetti, M.; Karring, T. Long-term stability of autogenous bone grafts following combined appli-cation with guided bone regeneration. *Clin. Oral Implants Res.* **2005**, *16*, 133–139. [CrossRef]
8. Rakhmatia, Y.D.; Ayukawa, Y.; Furuhashi, A.; Koyano, K. Fibroblast attachment onto novel titanium mesh membranes for guided bone regeneration. *Odontology* **2015**, *103*, 218–226. [CrossRef] [PubMed]
9. Di Stefano, D.A.; Greco, G.B.; Cinci, L.; Pieri, L. Horizontal-guided Bone Regeneration using a Titanium Mesh and an Equine Bone Graft. *J. Contemp. Dent. Pract.* **2015**, *16*, 154–162. [CrossRef] [PubMed]
10. De Moraes, P.H.; Olate, S.; De Albergaria-Barbosa, J.R. Maxillary Reconstruction Using rhBMP-2 and Titanium Mesh: Technical Note About the Use of Stereolithographic Model. *Int. J. Odontostomatol.* **2015**, *9*, 149–152. [CrossRef]
11. Sumida, T.; Otawa, N.; Kamata, Y.; Kamakura, S.; Mtsushita, T.; Kitagaki, H.; Mori, S.; Sasaki, K.; Fujibayashi, S.; Takemoto, M.; et al. Custom-made titanium devices as membranes for bone augmentation in implant treatment: Clinical application and the comparison with conventional titanium mesh. *J. Cranio-Maxillofac. Surg.* **2015**, *43*, 2183–2188. [CrossRef]
12. Saini, M.; Singh, Y.; Arora, P.; Arora, V.; Jain, K. Implant biomaterials: A comprehensive review. *World J. Clin. Cases* **2015**, *3*, 52–57. [CrossRef] [PubMed]
13. Ciocca, L.; Ragazzini, S.; Fantini, M.; Corinaldesi, G.; Scotti, R. Work flow for the prosthetic rehabilitation of atrophic patients with a minimal-intervention CAD/CAM approach. *J. Prosthet. Dent.* **2015**, *114*, 22–26. [CrossRef] [PubMed]
14. Al-Radha, A.S.D.; Dymock, D.; Younes, C.; O'Sullivan, D. Surface properties of titanium and zirconia dental implant materials and their effect on bacterial adhesion. *J. Dent.* **2012**, *40*, 146–153. [CrossRef] [PubMed]
15. Ponsonnet, L.; Reybier, K.; Jaffrezic, N.; Comte, V.; Lagneau, C.; Lissac, M.; Martelet, C. Relationship between surface properties (roughness, wettability) of titanium and titanium alloys and cell behaviour. *Mater. Sci. Eng. C* **2003**, *23*, 551–560. [CrossRef]
16. Elias, C.N.; Oshida, Y.; Lima, J.H.C.; Muller, C.A. Relationship between surface properties (roughness, wettability and morphology) of titanium and dental implant removal torque. *J. Mech. Behav. Biomed. Mater.* **2008**, *1*, 234–242. [CrossRef] [PubMed]
17. Le Guehennec, L.; Soueidan, A.; Layrolle, P.; Amouriq, Y. Surface treatments of titanium dental implants for rapid osseointegration. *Dent. Mater.* **2007**, *23*, 844–854. [CrossRef]
18. Dank, A.; Aartman, I.H.A.; Wismeijer, D.; Tahmaseb, A. Effect of dental implant surface roughness in patients with a history of periodontal disease: A systematic review and meta-analysis. *Int. J. Implant. Dent.* **2019**, *5*, 1–11. [CrossRef] [PubMed]
19. Rosales-Leal, J.I.; Rodríguez-Valverde, M.A.; Mazzaglia, G.; Ramón-Torregrosa, P.J.; Diaz Rodriguez, L.; García-Martínez, O.; Vallecillo-Capilla, M.; Ruiz, C.; Cabrerizo-Vílchez, M.A. Effect of roughness, wettability and morphology of engineered tita-nium surfaces on osteoblast-like cell adhesion. *Colloids Surf. A Physicochem. Eng. Asp.* **2010**, *365*, 222–229. [CrossRef]
20. Revilla-León, M.; Özcan, M. Additive Manufacturing Technologies Used for 3D Metal Printing in Dentistry. *Curr. Oral Health Rep.* **2017**, *4*, 201–208. [CrossRef]
21. Ciocca, L.; Fantini, M.; De Crescenzio, F. Direct metal laser sintering (DMLS) of a customized titanium mesh for pros-thetically guided bone regeneration of atrophic maxillary arches. *Med. Biol. Eng. Comput.* **2011**, *49*, 1347–1352. [CrossRef] [PubMed]
22. Hartmann, A.; Seiler, M. Minimizing risk of customized titanium mesh exposures—A retrospective analysis. *BMC Oral Health* **2020**, *20*, 36. [CrossRef]
23. Otawa, N.; Sumida, T.; Kitagaki, H.; Sasaki, K.; Fujibayashi, S.; Takemoto, M.; Nakamura, T.; Yamada, T.; Mori, Y.; Matsushita, T. Custom-made titanium devices as membranes for bone augmentation in implant treatment: Modeling accuracy of titanium products constructed with selective laser melting. *J. Cranio-Maxillofac. Surg.* **2015**, *43*, 1289–1295. [CrossRef] [PubMed]
24. Trevisan, F.; Calignano, F.; Aversa, A.; Marchese, G.; Lombardi, M.; Biamino, S.; Ugues, D.; Manfredi, D. Additive manufacturing of titanium alloys in the biomedical field: Processes, properties and applications. *J. Appl. Biomater. Funct. Mater.* **2018**, *16*, 57–67. [CrossRef]
25. Inoue, K.; Nakajima, Y.; Omori, M. Reconstruction of the alveolar bone using bone augmentation with selective laser melting titanium mesh sheet: A report of 2 cases. *Implant Dent.* **2018**, *27*, 602–607. [CrossRef]
26. Ortuğ, G. A new device for measuring mastication force (Gnathodynamometer). *Ann. Anat. Anat. Anz.* **2002**, *184*, 393–396. [CrossRef]
27. Shan, X.-F.; Chen, H.-M.; Liang, J.; Huang, J.-W.; Cai, Z.-G. Surgical Reconstruction of Maxillary and Mandibular Defects Using a Printed Titanium Mesh. *J. Oral Maxillofac. Surg.* **2015**, *73*, 1437–e1. [CrossRef] [PubMed]
28. Ciocca, L.; Lizio, G.; Baldissara, P.; Sambuco, A.; Scotti, R.; Corinaldesi, G. Prosthetically CAD-CAM–Guided Bone Augmentation of Atrophic Jaws Using Customized Titanium Mesh: Preliminary Results of an Open Prospective Study. *J. Oral Implant.* **2018**, *44*, 131–137. [CrossRef]
29. Cruz, N.; Martins, M.I.; Santos, J.D.; Gil Mur, J.; Tondela, J.P. Surface Comparison of Three Different Commercial Custom-Made Titanium Meshes Produced by SLM for Dental Applications. *Materials* **2020**, *13*, 2177. [CrossRef]